Coilopt, free boundary pies and island healing

S.R.Hudson, D.A.Monticello, A. Reiman,
D. J. Strickler, L. A. Berry, S. P. Hirshman,
A. Boozer
shudson@pppl.gov

December 18, 2000

Abstract

- A finite parameterization of the coils is varied to optimize free boundary PIES calculations with respect to island content and edge deformation.
- Results are shown that indicate general success of the island healing approach.

1 A set independent variables $\boldsymbol{x}$ is selected.

- Coils lie on a winding surface :

$$R = \sum_j r_j \cos(m_j\theta + n_j N\phi), \qquad Z = \sum_j z_j \sin(m_j\theta + n_j N\phi) \tag{1}$$

- The ith coil has toroidal variation :

$$\phi_i = \phi_{i0} + \sum_k \left[\phi^c_{i,k}\cos(k\theta') + \phi^s_{i,k}\sin(k\theta')\right], \qquad \theta' = \theta + \sum_j \rho^s_{i,j}\sin(j\theta) \tag{2}$$

- A chosen subset of $\{\phi^c_{i,k}, \phi^s_{i,k}, \rho^s_{i,j}\}$ form a vector of independent parameters $\boldsymbol{x}$ that will be varied to *zero-minimize* a vector function.
- N independent parameters.

2 A vector function $\boldsymbol{B}$ to be targeted is defined.

- The vector function to be targeted ...

$$\boldsymbol{B} = \begin{pmatrix} E \\ B_{n_1 m_1} \\ B_{n_2 m_2} \\ B_{n_3 m_3} \\ \vdots \end{pmatrix} = \begin{pmatrix} \text{edge deformation } E = \sum_i (\rho_i - \rho_0)^2 / N \geq 0 \\ (n_1, m_1) \text{ resonant field at } \iota = N m_1 / n_1 \\ (n_2, m_2) \text{ resonant field at } \iota = N m_2 / n_2 \\ (n_3, m_3) \text{ resonant field at } \iota = N m_3 / n_3 \\ \vdots \end{pmatrix} \tag{3}$$

- The edge deformation E and resonant fields B_{nm} are calculated using PIES. For each coil set $\boldsymbol{x}$, 20 PIES iterations from an initial VMEC equilibrium are performed.
- If the chosen independent parameters provide sufficient freedom the B_{nm}'s may be zeroed. The phase of the island depends on the sign on B_{nm}.
- E must be minimized; ideally $E \to 0$ but practically this is impossible.
- E and B_{nm} have different units, different magnitude and need to be appropriately scaled.
- M constraint equations.

3 The resonant fields are calculated using PIES diagnostics.

- A diagnostic calculating resonant fields has been included in PIES. Resonant fields are determined using quadratic-flux minimizing surfaces.
- The solid lines are the quadratic-flux minimizing surface passing directly through the (1,5) island chain and the estimation of the separatrix.
- The arrows indicate the action gradient $\sim$ resonant field.
- A Poincaré plot shows 3 trajectories with dots.

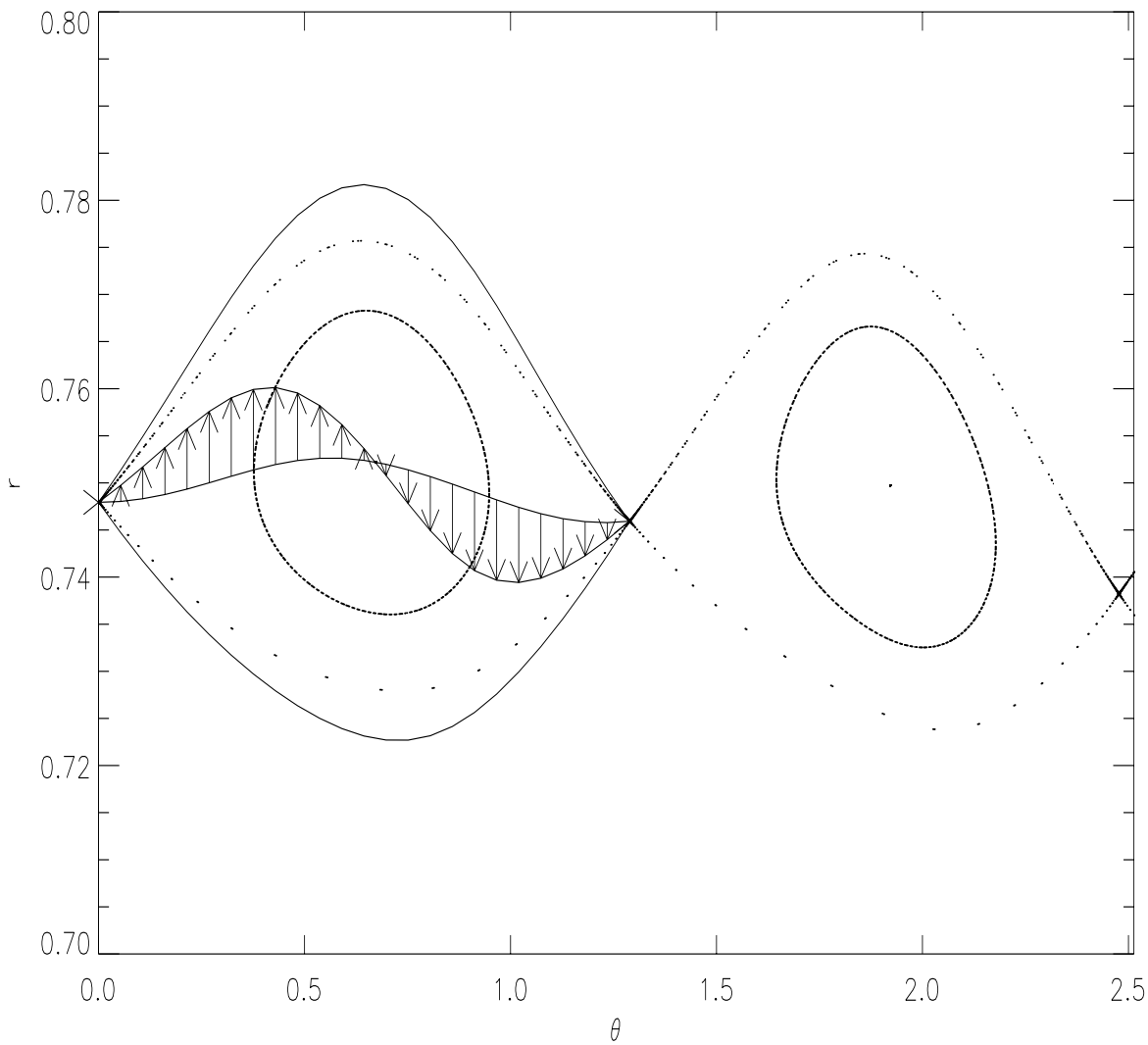

Figure 1: illustration of resonant field at (1,5) resonant surface

4 The derivative matrix $\boldsymbol{C}$ is constructed.

- The linear relationship is described by and $M \times N$ matrix $\boldsymbol{C}$ where typically $M < N$.

$$\boldsymbol{B}(\boldsymbol{x}) = \boldsymbol{B}(\boldsymbol{x}_0) + \boldsymbol{C} \cdot \boldsymbol{\delta x} + \ldots \tag{4}$$

- The jth column of $\boldsymbol{C}$ is determined with a PIES calculation where the change in $\boldsymbol{B}$ is measured for a small change in x_j, thus $N + 1$ PIES calculations are required.
- $\boldsymbol{C}$ may be represented using singular value decomposition

$$\boldsymbol{C} = \mathbf{U}\mathbf{w}\mathbf{V}^{\mathbf{T}} \tag{5}$$

  where $\mathbf{w}$ is a diagonal matrix of the singular values.
- There will be at least $N - M$ zero singular values associated with the nullspace.
- If $\boldsymbol{x}$ is near the minimum of E, an additional singular value will be very small. Similarly if a particular B_{nm} cannot be zeroed.

5 The solution is calculated via iteration.

- The solution $\boldsymbol{B} = 0$ is located through iteration :

$$\boldsymbol{\delta x}_i = -\boldsymbol{C}^{-1} \cdot \boldsymbol{B}(\boldsymbol{x}_i) \qquad ; \qquad \boldsymbol{x}_{i+1} = \boldsymbol{x}_i + \boldsymbol{\delta x}_i \tag{6}$$

  where the inverse $\boldsymbol{C}^{-1}$ is approximated

$$\boldsymbol{C}^{-1} = \mathbf{V} \cdot [diag(1/w_j)] \cdot \mathbf{U}^{\mathbf{T}} \tag{7}$$

  where $1/w_j$ is replaced by zero if $|w_j|/|w_{\max}| < \epsilon$.

- Broyden's method is used to update $\boldsymbol{C}$ during the iterations according to

$$\boldsymbol{C}_{i+1} = \boldsymbol{C}_i + \frac{(\boldsymbol{\delta B}_i - \boldsymbol{C}_i \boldsymbol{\delta x}_i) \otimes \delta \mathbf{x_i}}{\delta \mathbf{x_i} \cdot \delta \mathbf{x_i}} \tag{8}$$

- A simple acceptance test is used : if $|B_{i+1}|/|B_i| > 1$ then $\boldsymbol{\delta x}_i \rightarrow \boldsymbol{\delta x}_i/2$.

6 The initial coil set gives islands/edge deformation.

- A Poincaré plot of the initial configuration shows that the edge and the (1,5) island clearly need targeting.

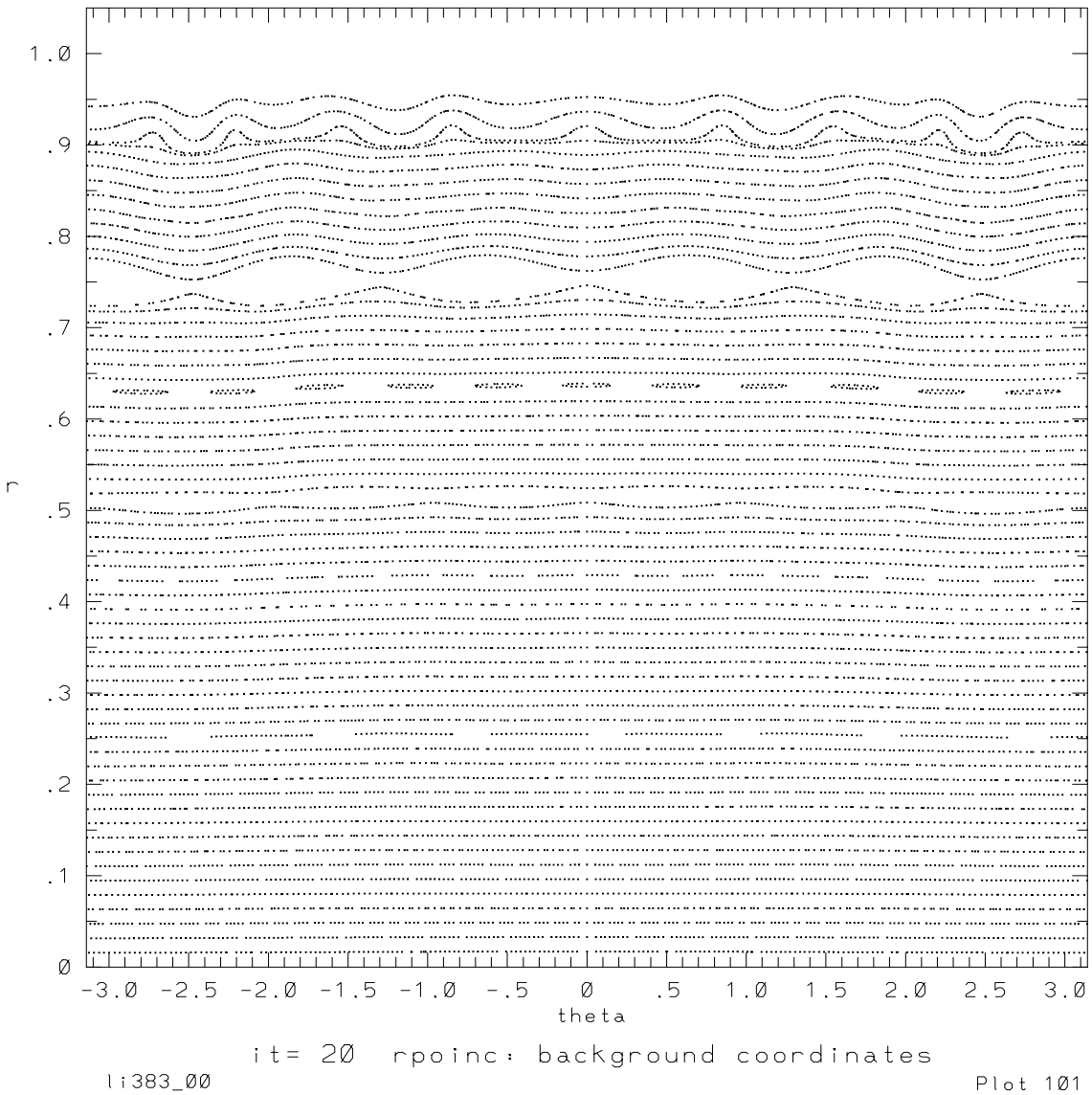

Figure 2: Poincaré plot for initial coil set

7 The rotational transform profile identifies problems.

- The ι profile shows the low order rational surfaces $\iota = 3/5$, $3/6$ and $6/9$ are present.
- The edge deformation may be due to the 2/9 resonance.

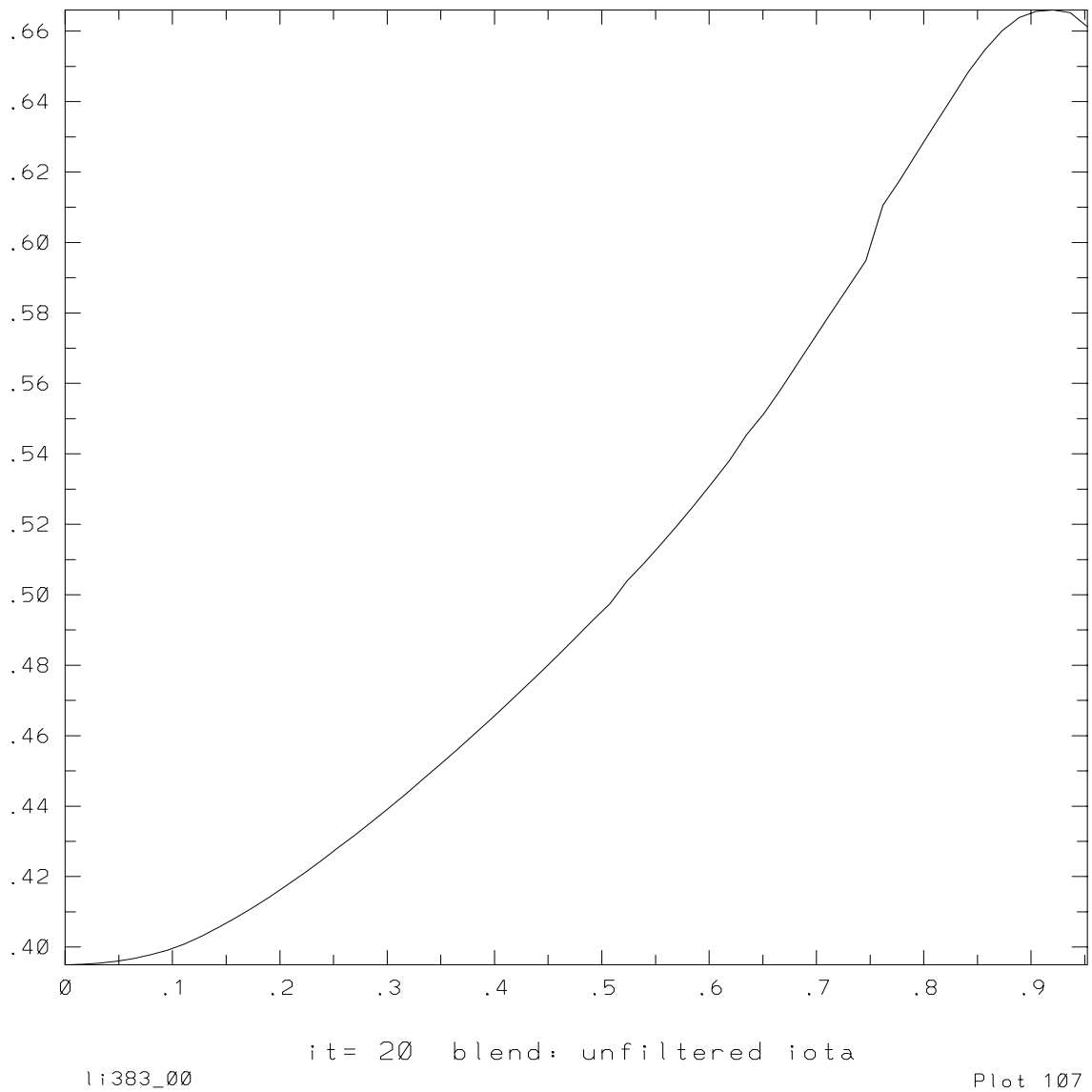

Figure 3: rotational transform for initial coil set

8 After more PIES iterations, surfaces deteriorate.

- The Poincaré plot of initial coil set after more iterations shows chaos and islands growing.

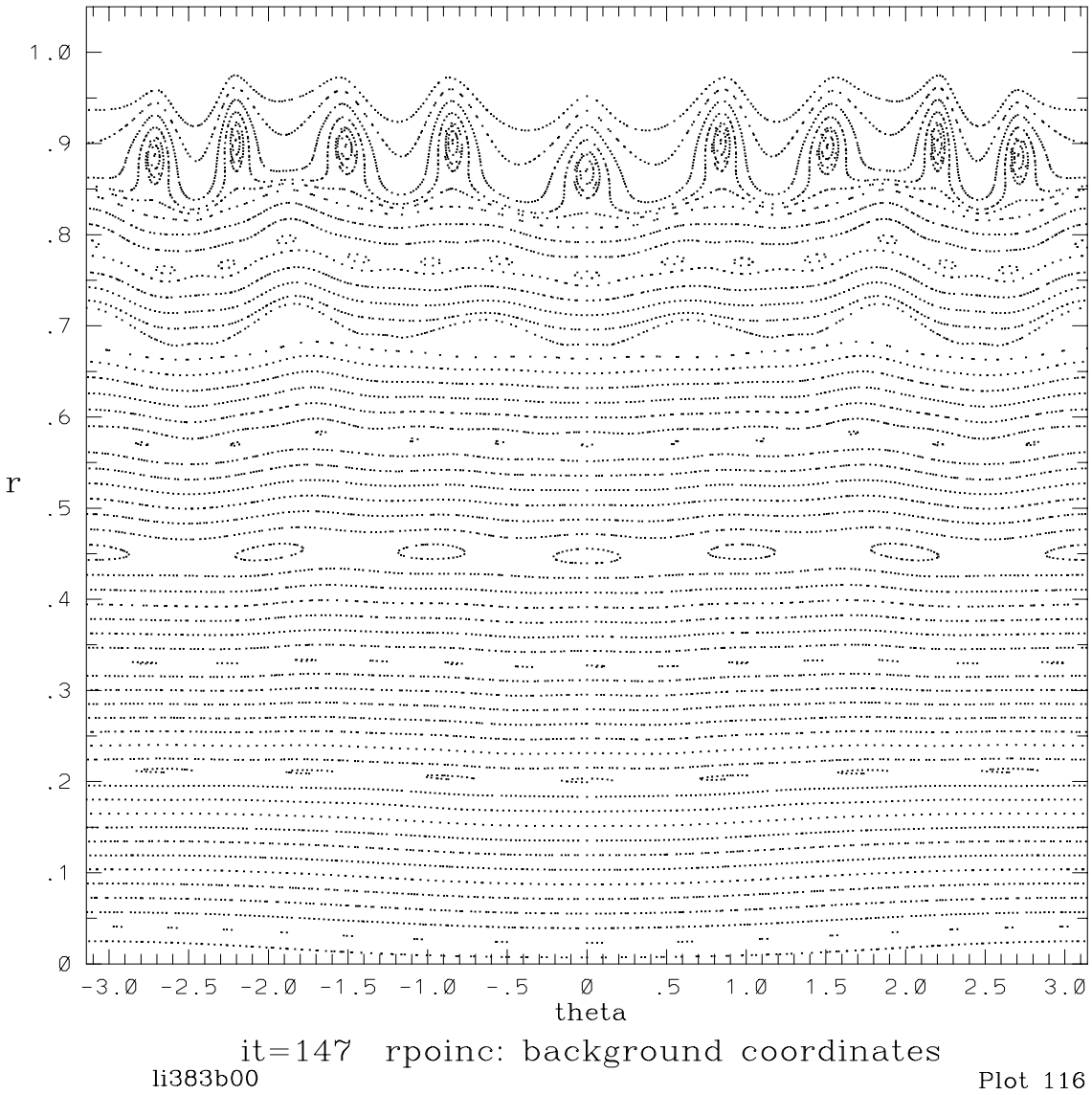

Figure 4: Poincaré plot for initial coil set after more PIES iterations

9 Attempt A :

- The edge deformation and the (1,5) and (1,6) resonant fields are targeted.
- The 5,6, and 10 cosine and sine modes of all coils are varied.
- The coupling matrix is a 3×21 matrix ...

$$\begin{pmatrix} \delta E \\ \delta B_{1,5} \\ \delta B_{1,6} \end{pmatrix} = \begin{pmatrix} \\ \\ \\ \end{pmatrix} \begin{pmatrix} \delta\phi^c_{1,5} \\ \delta\phi^s_{1,5} \\ \delta\phi^c_{1,6} \\ \delta\phi^s_{1,6} \\ \delta\phi^c_{1,10} \\ \delta\phi^s_{1,10} \\ \delta\phi^c_{2,5} \\ \delta\phi^s_{2,5} \\ \delta\phi^c_{2,6} \\ \delta\phi^s_{2,6} \\ \delta\phi^c_{2,10} \\ \delta\phi^s_{2,10} \\ \delta\phi^c_{3,5} \\ \delta\phi^s_{3,5} \\ \delta\phi^c_{3,6} \\ \delta\phi^s_{3,6} \\ \delta\phi^c_{3,10} \\ \delta\phi^s_{3,10} \\ \delta\phi^s_{4,5} \\ \delta\phi^s_{4,6} \\ \delta\phi^s_{4,10} \end{pmatrix} \tag{9}$$

$$\boldsymbol{C}$$

10 Attempt A : Convergence seems satisfactory.

- The iterative optimization shows good reduction of target function and decrease in successive step size.

		E	$B_{1,5}$	$B_{1,6}$	$\lvert B\rvert$	$\lvert\delta x\rvert$
0		1.00000	1.00000	1.00000	1.73205	0.00603
1		0.30671	0.09258	−1.10797	1.15336	0.00250
2		0.27794	0.04495	0.01287	0.28185	0.00169
3		0.24814	0.00060	−0.05112	0.25335	0.00002
4		0.24614	−0.00381	−0.05630	0.25252	

(10)

- The evolution of the singular values indicates if zero or minimum is found; w_3 becomes small suggesting solution approaches minimum of E.

		w_1	w_2	w_3
0		541.30259	135.96148	288.70348
1		625.12927	139.88416	244.89716
2		641.51869	140.24710	166.63104
3		641.42930	148.21241	9.57702

(11)

11 Attempt A : Edge and surfaces are healed.

- The Poincaré plot of produced by attempt A healed coil set shows significant improvement of surfaces and reduction of edge deformation.

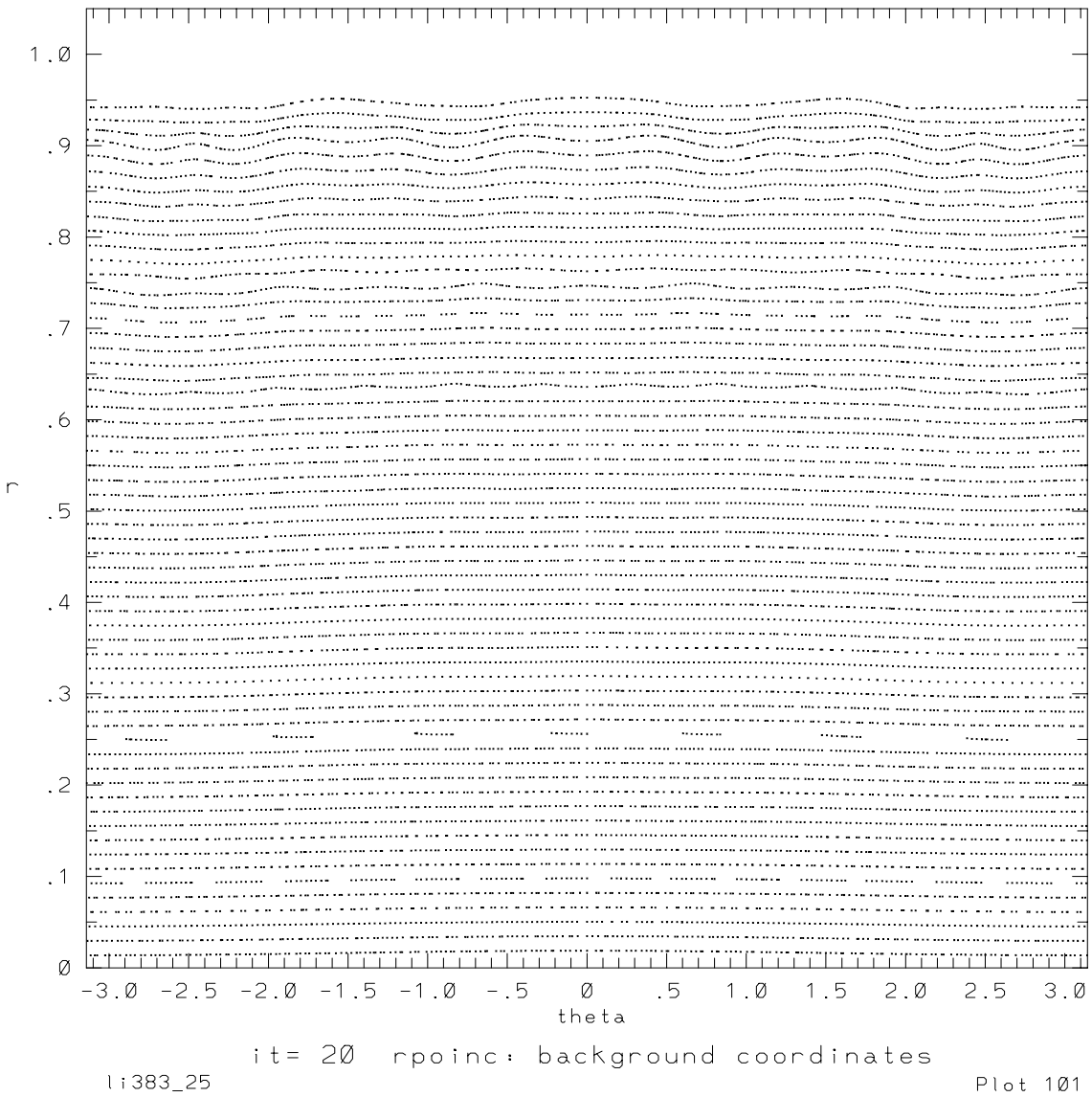

Figure 5: Poincaré plot corresponding to healed coil set

12 Attempt A : Rotational transform profile unchanged.

- The rotational transform produced by attempt A healed coil set is similar to original.

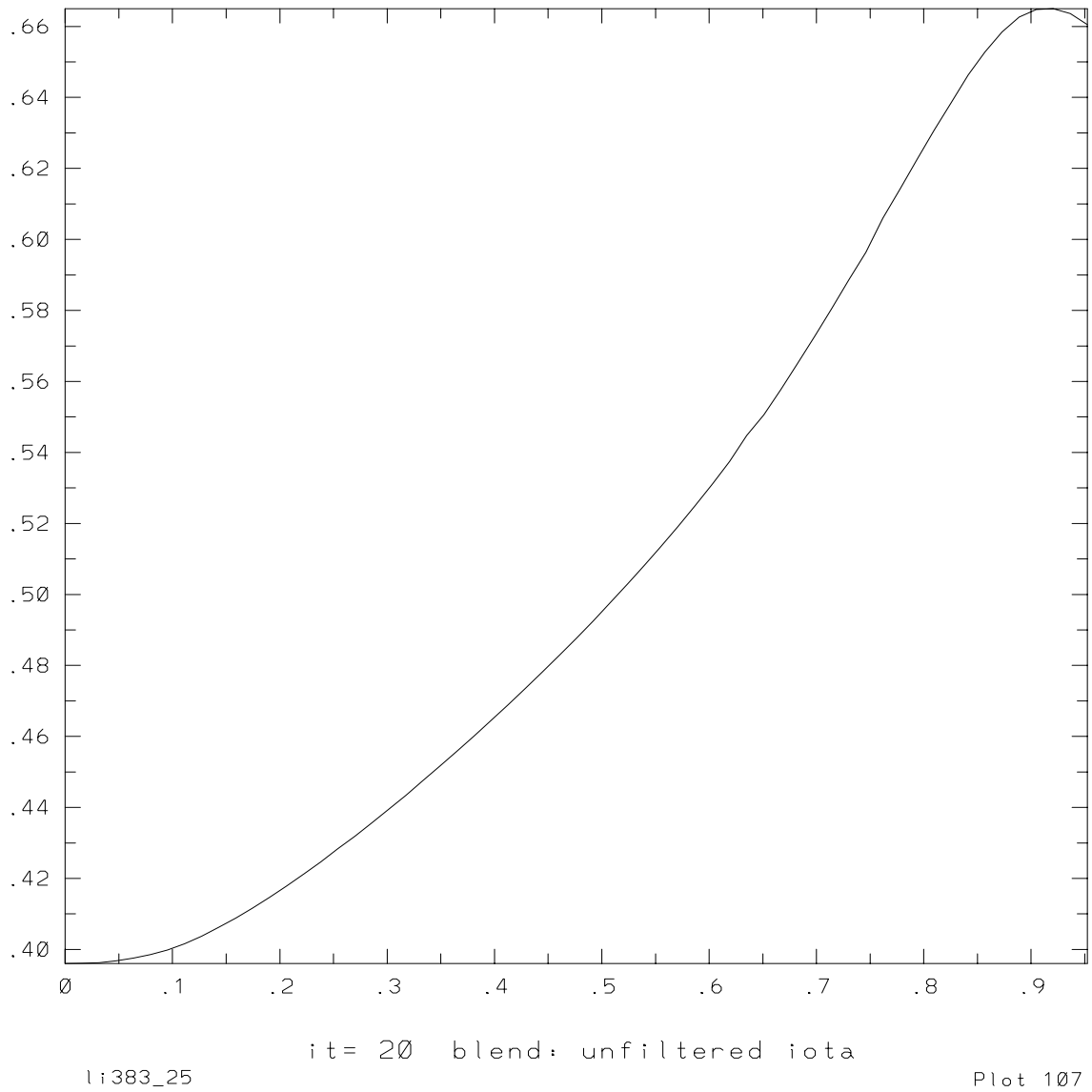

Figure 6: rotational transform corresponding to healed coil set

13 Attempt A : PIES convergence test in progress.

- The Poincaré plot of attempt A healed coil set after more PIES iterations shows slight increase island of island content and edge deformation (as compared to 20 iterations) but improved compared to original.

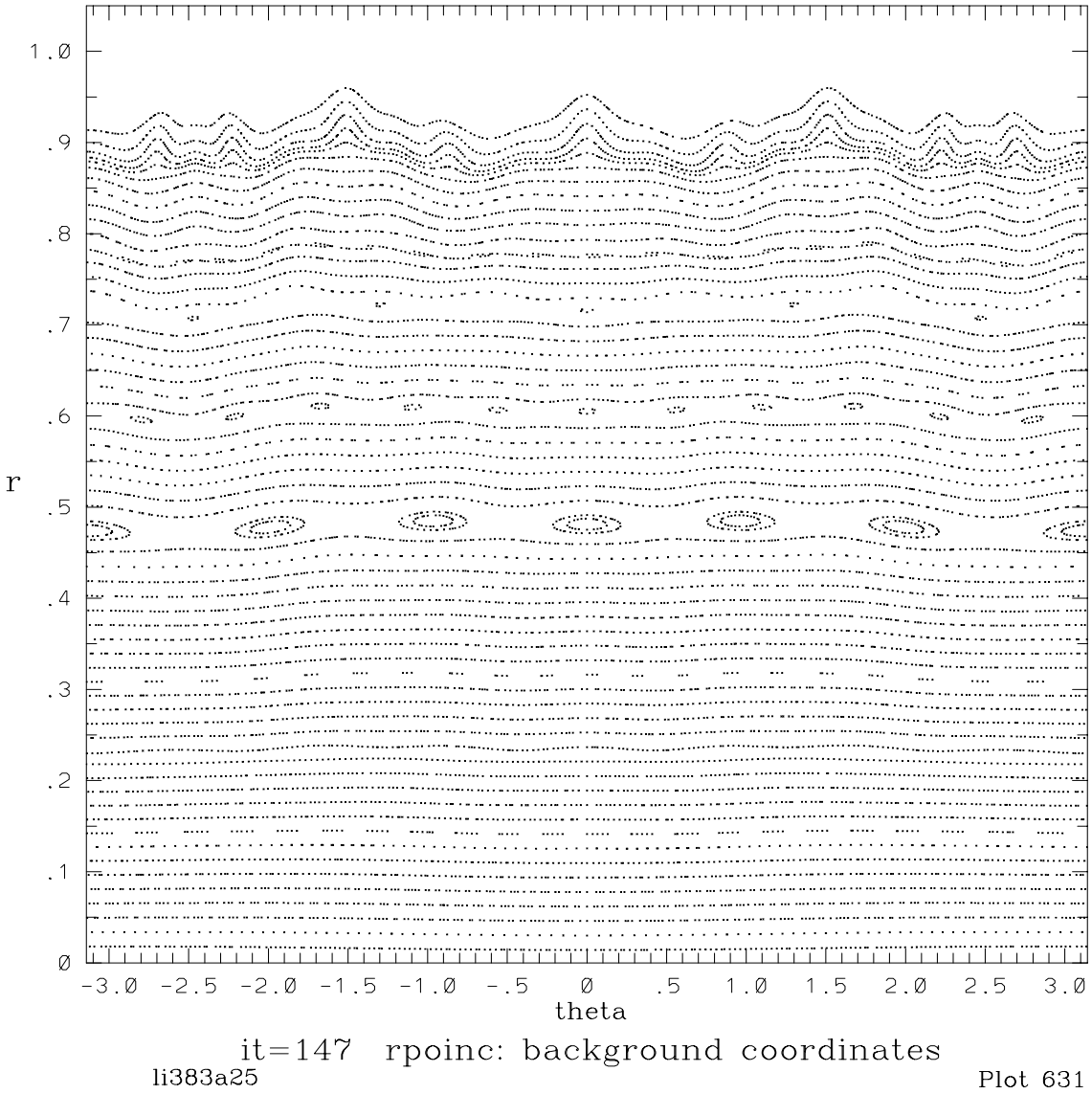

Figure 7: Poincaré plot corresponding to healed coil set after more PIES iterations

14 Attempt B : PIES convergence test in progress.

- Attempt B is similar but reduced set of target resonances

$$\boldsymbol{B} = \begin{pmatrix} E \\ \delta B_{1,5} \\ \delta B_{1,6} \end{pmatrix} \tag{12}$$

- The Poincaré plot of attempt B healed coil set after more PIES iterations ...

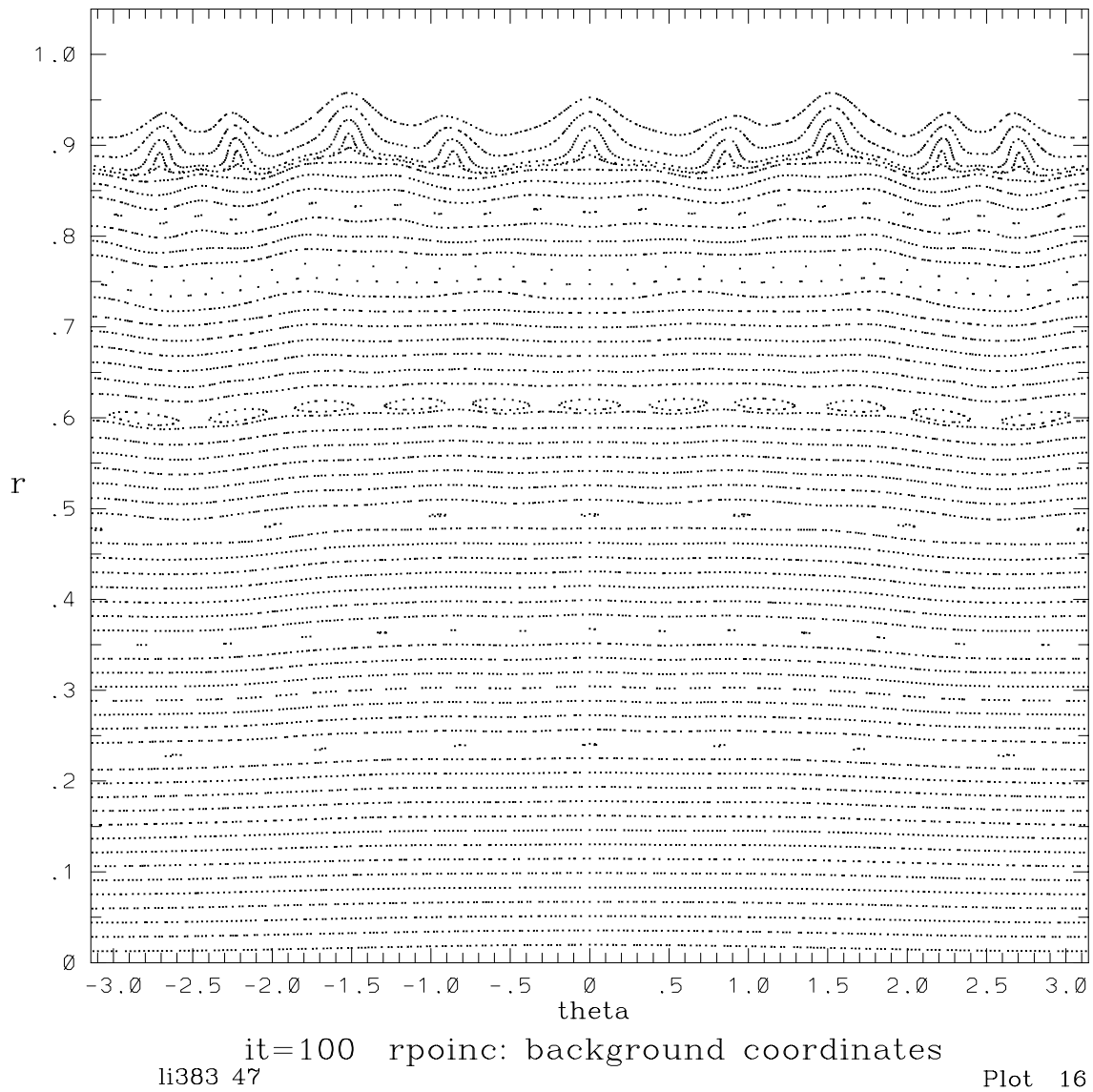

Figure 8: Poincaré plot corresponding to healed coil set after more PIES iterations

15 Comments.

- Island healing and edge flattening after 20 PIES iterations are obtained with the algorithm.
- Being based on PIES calculations, this work is inevitably slow. To confirm that converged PIES equilibriums maintain the good surfaces is even slower.
- 'Dynamical' modification of the coil set during PIES runs is presently being considered.
- There is a large dimensionality nullspace which should be utilized to optimize physics and engineering constraints.
- The full coupling matrix will indicate sensitivities of edge deformation/island content on coil parameters or equivalently sensitivity on spectrum of coil field on control surface.
- Success of the numerical procedure requires care with
  - δx_i where $x_i \rightarrow x_i + \delta x_i$ is used to calculate partial derivatives for $\boldsymbol{C}$;
  - ϵ used to ignore small singular values;
  - choice of independent parameters $\{\phi^c_{i,k}, \phi^s_{i,k}, \rho^s_{i,j}\}$ and choice of B_{nm}'s;
  - the scaling of $\boldsymbol{B}$;
  - at which iterations should $\boldsymbol{C}$ be modified;